Appendix

Lucarelli, J., Carroll, H., Elliott, B., Coplen, T., Eagle, R., Tripati, A. Equilibrated gas and carbonate standard-derived paired clumped isotope (Δ_{47} and Δ_{48}) values on the absolute reference frame, Rapid Communications in Mass Spectrometry

Term	Definition	Abbreviation
Estimated marginal mean	Groupwise mean calculated from a model fit to data	EMM
Ordinary marginal mean	Groupwise mean calculated directly from data	OMM
Standard deviation	σ (sigma)	SD
Standard error	Standard deviation divided by the square root of the number of observations: $\frac{\sigma}{\sqrt{n}}$	SE

A.1 Background of statistical methods used

For Δ_{47} and Δ_{48} quality assurance, we adapted screening criteria used in other disciplines, implementing kernel density estimation as a statistical technique for use with clumped isotope data. Kernel density estimation has a broad range of research applications, including economics[1], ecology[2], climate modeling[3], weather forecasting[4], and manufacturing controls[5], among others. We chose this approach for its relative simplicity of calculation and ability to eliminate extreme values from the dataset. Extreme values must be eliminated prior to employing a cut at 3σ because the standard deviation may be strongly affected by their presence. For each sample, we calculated a kernel density estimate using the generic S3 method 'density' included in base R's stats package.[6] In quality screening of clumped isotope data, a nonparametric approach, such as kernel density estimation, is preferred because we often have no *a priori* knowledge of the statistical properties of the raw clumped isotope replicate pool. In density estimation, a weighting function, known as a kernel, is applied to the data; in the R implementation of kernel density estimation, the default is to use a normally distributed (Gaussian) kernel, K, applied to a variable, u. The normal distribution takes the form:

$$K(u) = \frac{1}{\sqrt{2\pi}} e^{\frac{-1}{2}u^2}$$

The smoothing parameter, known as bandwidth, using the default normally distributed kernel, is set to equal the standard deviation of the kernel, or weighting function, itself.[6] The kernel then becomes a curve that integrates to 1 with the statistical properties:

$$\sigma^2(K) = t^2K(t)dt$$

For a full explanation of bandwidth selection in nonparametric probability density estimation, see Sheather & Jones[7]; for a full explanation of kernel density estimation as implemented in R, see Deng & Wickham[8].

Kernel density estimation is used to examine the underlying probability density function (PDF) for a given variable. Each clumped isotope sample value is not a single definite point, due to the uncertainty inherent in replicate measurements, but is rather a finite probable range of values. This can be visualized as a peak where the most probable values for a given variable cluster together to produce the peak's maxima; this is the probability density function. This is similar to the way in which histograms demonstrate data distributions based on counts (Figure 3A in main text). From the PDF peak for each standard, we found the nearest minima, or least probable values of the possible range, on either side of the maxima, or most probable value, and defined those minima as the initial cutpoints for exclusion (Figure 3B). In cases where the PDF revealed a double peak or a shoulder at least a third as high as the true maxima, we used the second nearest minima or left/right minima according to the shape of the density peak. We chose a cutoff of 1/3 as high as the true maxima because it produced final Δ_{47} sample mean data in good agreement with data processed using other methods (Table S2).

The PDF-based exclusion method has been included as a custom function in a publicly available R script (available on GitHub at https://github.com/Tripati-Lab/Lucarelli-et-al; all code and data will be permanently archived on Dryad upon acceptance for publication and a static link make available here), and instructions for its use are given in the script. Hereafter, we refer to this statistical technique as the "PDF method" for the sake of brevity.

Following initial screening using the PDF method, we employed a 3σ exclusion which yielded results for Δ_{47} and Δ_{48} that were consistent across instruments. A Shapiro-Wilk test was used to determine whether the resulting data were consistent with a normal distribution.

A.1.1 Inter-instrumental comparisons and data pooling

Five mass spectrometer configurations (Table 2 in main text) were used to measure clumped isotopes in this study. To ensure it was appropriate to pool data produced using different mass spectrometer configurations, we performed statistical tests comparing individual sample mean values produced on each configuration and also the overall cumulative comparability of each configuration. To test for any differences between configurations that would preclude pooling data for analyses, we modeled final clumped isotope values by the additive effects of configuration and sample using a linear mixed effects model from package *nlme* version 3.1-152[9] after Upadhyay et al.[10] Linear mixed effects models provide a convenient extension to conventional linear models, in that they allow for both fixed effects (the independent variables) and random effects (additional variables which may affect the dependent variables, but which are not being explicitly modeled). The standard error of the final

clumped isotope replicate was included as a random effect in the model. Including SE as a random effect in the model is done to capture the effect of differences in precision from measurement to measurement, and account for them in the calculation of model coefficients. Standard error is considered a random effect instead of a fixed effect (i.e., a predictor or independent variable) because it is not constant across observations in a given dataset. Standard regression models, that is, fixed effects models, are more accurate when error is relatively uniform across observations. They carry the risk of being overly sensitive to random error in the dataset when it is not uniform, which leads to bias in estimating the relationship between the independent and dependent variables. Mixed effects models account for the non-uniform random error and reduce that risk. However, mixed effects models can produce bias if the error is entirely uncorrelated with the relationship between the independent and dependent variables. In practice, this is extremely unlikely. Models did not include samples that were run rarely on these instruments, and for which we have few replicates (ISTB-1, TB-1, TB-2, CIT Carrara, DH-2-10, DH-2-11, DH-2-12, DH-2-13, TV01, 47407 Coral, Spel-2-8-E, and 102-GC-AZ01).

Pairwise differences between configurations were then assessed using contrasts with adjustment for multiple comparisons from package *emmeans* version 1.5.4.[11] Estimated marginal means, used here for inter-instrumental comparisons, are preferred to ordinary marginal means because they control for differences in the number of analyses run on individual configurations. Marginal means are defined as the mean value of a given group. For example, an ordinary mean for the standard ETH-1 would be the mean calculated from all available replicates of ETH-1, without taking the instruments which produced them into account. By contrast, ordinary marginal means would consist of a separate mean value for ETH-1 for each of the mass spectrometers on which it was measured. These are reported throughout the manuscript wherever a mass spectrometer configuration is specified. Estimated marginal means, used here for inter-instrumental comparisons, are based on a model fit to the data, rather than the raw data. This has the effect of controlling for unequal numbers of observations per group, such that the final value for a given sample produced by an instrument which has an N = 50 is not downweighted relative to an instrument which has an N = 150. This is useful when comparing the values produced by one instrument to another, as unequal numbers of observations violate the assumptions of most parametric statistical tests and may lead to erroneous conclusions. As the estimated marginal means differ slightly from the more commonly reported ordinary marginal means, we use them strictly for inter-instrumental comparisons, and report ordinary marginal means throughout the rest of the manuscript. Data were pooled for further analyses only if there was no evidence of a statistically significant difference between configurations across any of the samples reported herein.

A.1.2 Statistical method implementation

This section contains step-by-step instructions with examples for working with the custom R script available at https://github.com/Tripati-Lab/Lucarelli-et-al. Note that the subset of data present here is unusually noisy for demonstration purposes, and more replicates are removed than what is typically observed in a real dataset. We chose this

subset so that users would be able to clearly follow our descriptions and visualize changes in the data distribution.

Samples or standards with multiple aliquots should be grouped. For example, many labs will utilize ETH-1. Aliquots included in this study are 1-4. If these are coded by aliquot number, such as ETH-1-1, ETH-1-2, etc., these should be grouped together and named ETH-1. As an example:

```
unique(data$Easotope_Name)
##  [1] "TV03"          "Veinstrom"     "Carmel Chalk"   "ETH-1-1"
##  [5] "ETH-2-1"       "ETH-3-1"       "ETH-4-1"        "Carrara Marble"
##  [9] "ETH-2-2"       "ETH-3-3"       "ETH-4-2"        "ETH-1-2"
## [13] "ETH-1-3"       "ETH-2-3"
```

We have multiple aliquots of ETH-1, ETH-2, ETH-3, and ETH-4. The rest of the samples/standareds are not given aliquot numbers. We only need to group the ETH standards. We use partial string matching for this purpose:

```
library(dplyr)

data <- data %>%
  mutate(Standard = case_when(
    !grepl("ETH", Easotope_Name) ~ Easotope_Name,
    grepl("ETH-1", Easotope_Name) ~ "ETH-1",
    grepl("ETH-2", Easotope_Name) ~ "ETH-2",
    grepl("ETH-3", Easotope_Name) ~ "ETH-3",
    grepl("ETH-4", Easotope_Name) ~ "ETH-4"
    )
  )
```

We now have standardized names as follows. Note that the original name is not overwritten - we add a new column and preserve the original designations.

```
unique(data$Standard)
## [1] "TV03"          "Veinstrom"     "Carmel Chalk"   "ETH-1"
## [5] "ETH-2"         "ETH-3"         "ETH-4"          "Carrara Marble"
```

Finding initial cutpoints

Kernel density estimation is used to find initial cutpoints.
When there is a singular peak, the findCutpoints function is employed as follows:

```
ETH2_cuts <- findCutpoints(data$D48CDES_Final[data$Standard == "ETH-2"])
```

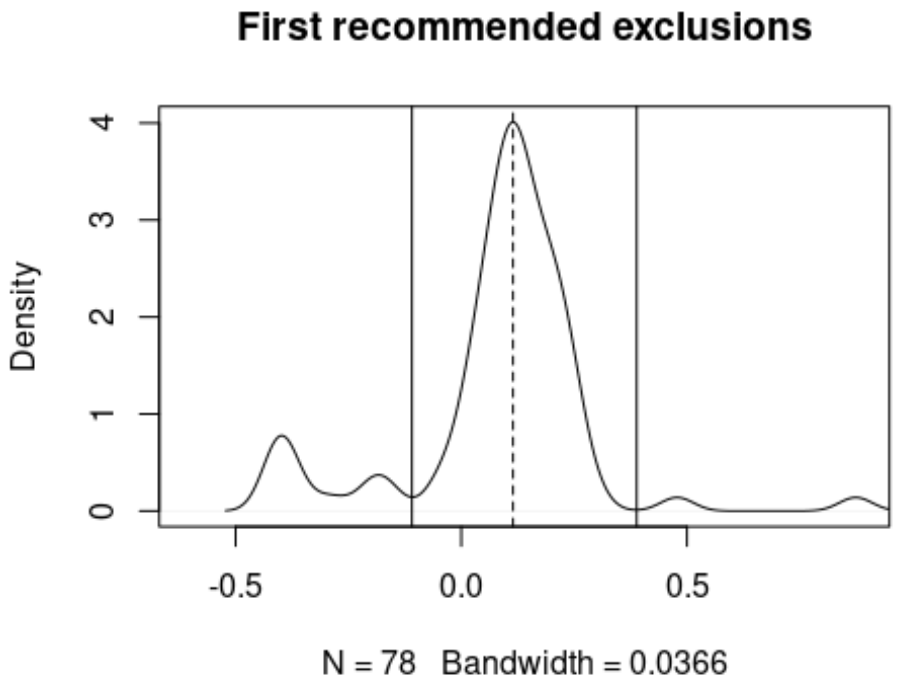

The recommended cuts (nearest minima on either side of the maxima) are marked in solid black vertical lines. In this case, recommended cuts are:

```
ETH2_cuts[1]
## [1] -0.1093086
ETH2_cuts[2]
## [1] 0.3886321
```

Note that the functions do not round values, as we wish to avoid accumulating rounding error.

Those suggested cuts are stored in the object **ETH2_cuts**, then applied to the raw data as follows:

```
ETH2_firstcut <- data$D48CDES_Final[data$Standard == "ETH-2" &
                        data$D48CDES_Final >= ETH2_cuts[1] &
                        data$D48CDES_Final <= ETH2_cuts[2] ]
```

Following the exclusion of extreme values, our data are as follows:

```
mean(ETH2_firstcut)
## [1] 0.1275455
sd(ETH2_firstcut)
## [1] 0.07563763
length(ETH2_firstcut)
## [1] 66
```

Final exclusions

A visual representation of options for the final exclusion:

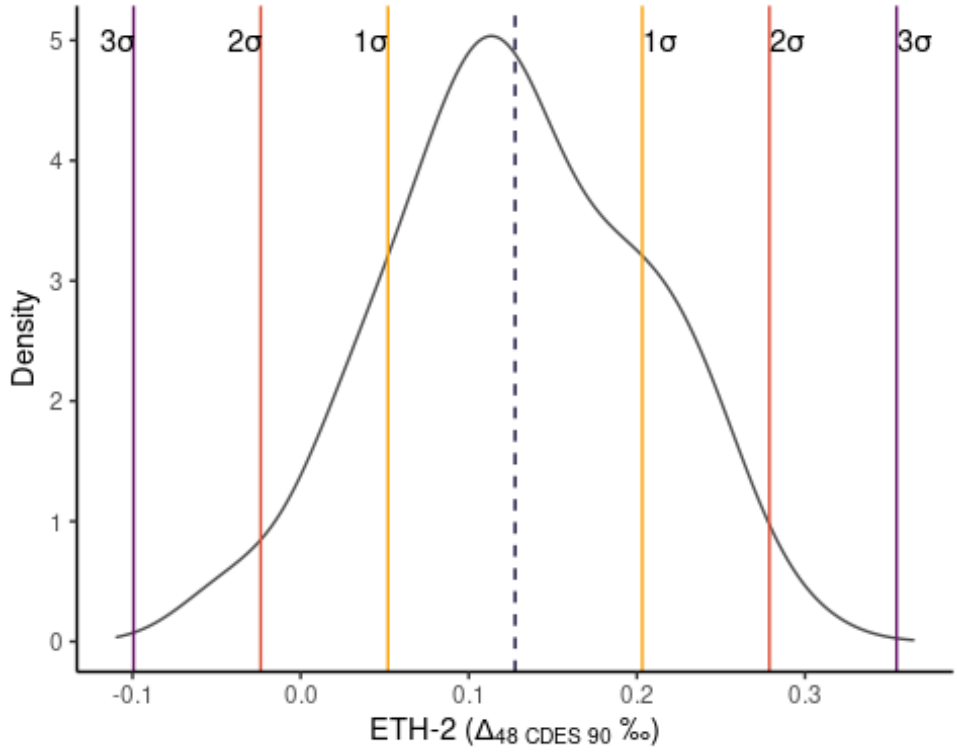

We then employ a 3σ exclusion (outermost pair of solid vertical lines in purple) to complete the quality control process:

```
ETH2_secondcut <- ETH2_firstcut[ETH2_firstcut >= (mean(ETH2_firstcut)-
(3*sd(ETH2_firstcut))) &
                          ETH2_firstcut <= (mean(ETH2_firstcut)+(3*sd(ETH2_firstcut)))]

mean(ETH2_secondcut)
## [1] 0.1275455
sd(ETH2_secondcut)
## [1] 0.07563763
length(ETH2_secondcut)
## [1] 66
```

These final cuts are then applied to the full dataset:

```
ETH2_final <- data[data$Standard == "ETH-2" &
                   data$D48CDES_Final >= range(ETH2_secondcut)[1] &
                   data$D48CDES_Final <= range(ETH2_secondcut)[2],]
```

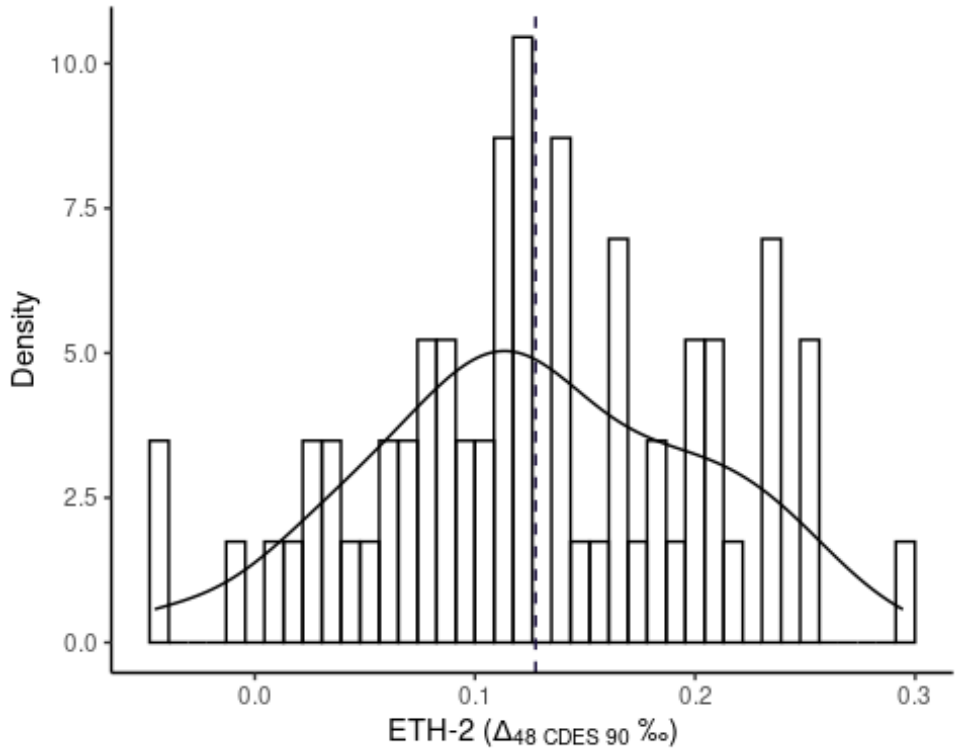

We test for normality of the final dataset as follows:

```
shapiro.test(ETH2_final$D48CDES_Final)
##
##  Shapiro-Wilk normality test
##
## data:  ETH2_final$D48CDES_Final
## W = 0.98847, p-value = 0.8011
```

The final data are normally distributed, so we are satisfied with the 3σ exclusion.

Data screening when there are double peaks or shoulders

We provide an additional set of functions to address more complex situations. For double or shouldered peaks, the nearest minima will be inaccurate. Where a second peak or shoulder is approximately a third as high as the highest peak, these data should be included in the initial cut. This is most likely to occur when replicate pools are relatively small or when older instrumentation, such as a Thermo Finnigan MAT 253, is used to measure Δ_{48}.

An example where the second peak is on the left hand side of the maxima:

```
findCutpoints(data2$D47CDES_90[data2$Standard == "IAEA-C2"])
```

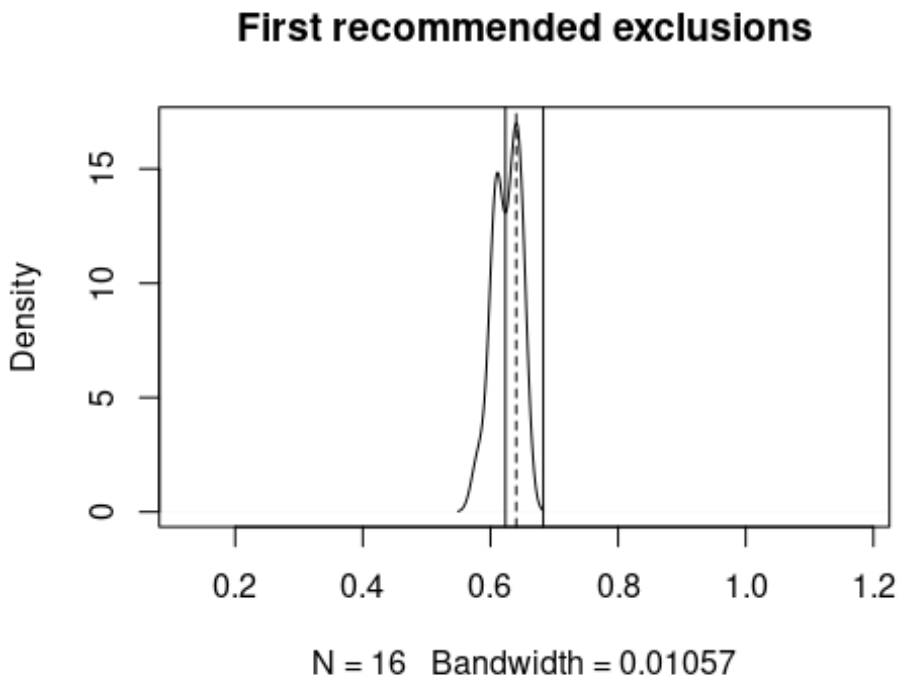

This will require the function findCutpointsLeftShoulder:

```
findCutpointsLeftShoulder(data2$D47CDES_90[data2$Standard == "IAEA-C2"])
```

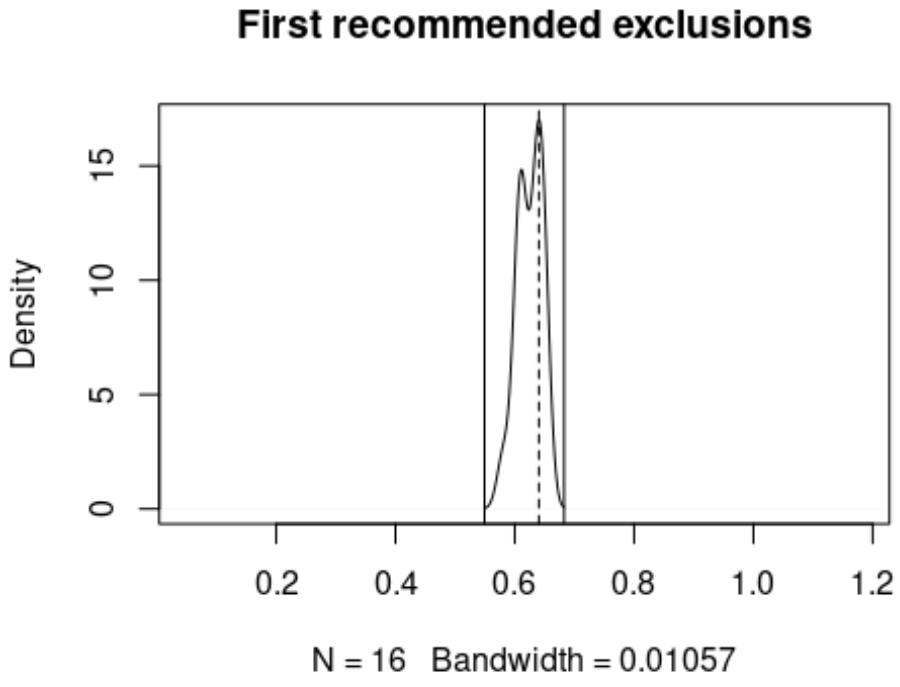

The findCutpointsRightShoulder function is provided for cases such as the example below:

```
findCutpointsRightShoulder(data2$D47CDES_Final[data2$Standard == "102-GC-AZ01"])
```

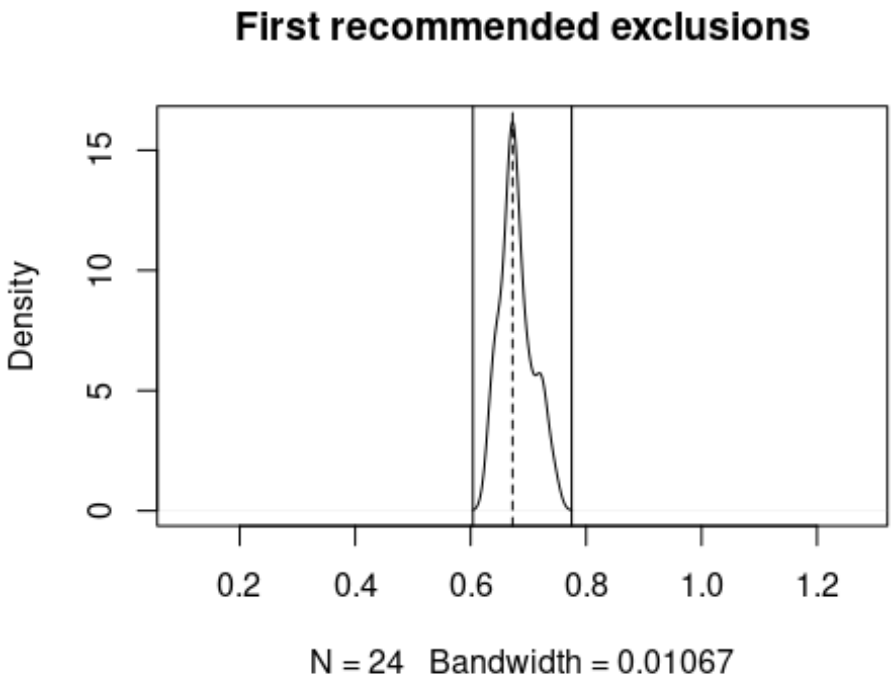

We provide the function findCutpointsDouble for peaks with shoulders on both sides:

```
findCutpointsDouble(data3$D48CDES_Final[data3$Standard == "ETH-1"])
```

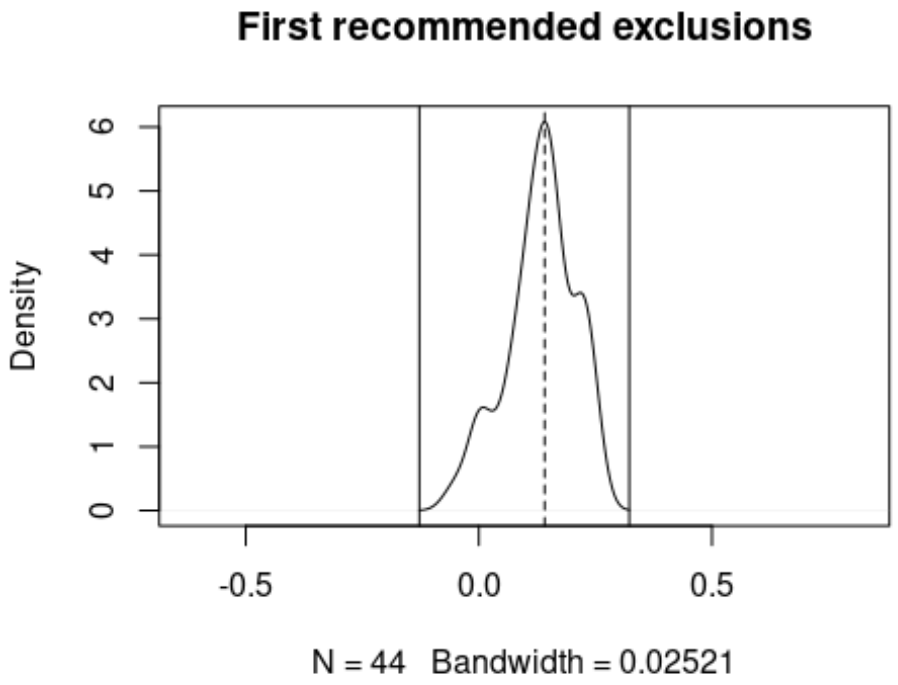

Following the initial exclusions, we then proceed with the final exclusions as described above.

A.2 Regression-form acid digestion fractionation factors, $\Delta^*_{63\text{-}47}$ and $\Delta^*_{64\text{-}48}$

Model calculations from Guo et al.[12] predicted that acid digestion fractionation factors (AFFs) for when calcite mineral is digested in phosphoric acid, $\Delta^*_{63\text{-}47}$ and $\Delta^*_{64\text{-}48}$, should depend on the Δ_{63} and Δ_{64} values of the reactant carbonate, respectively. Here, to calculate this dependence, nonlinear regressions of the theoretical model equilibrium Δ_{63} or Δ_{64} and temperature[13,14] were used to determine theoretical equilibrium Δ_{63} and Δ_{64} values for the precipitation temperature of Devils Hole calcite at 33.7 ^{o}C[15] ($\Delta_{63} \approx 0.3707$ ‰; $\Delta_{64} \approx 0.1092$ ‰) and ETH-1 and ETH-2 at 600 ^{o}C[16] ($\Delta_{63} \approx 0.0179$ ‰; $\Delta_{64} \approx 0.0022$ ‰). The experimentally determined Δ_{47} and Δ_{48} values for DH-2 average and the pooled average of ETH-1 and ETH-2 were subtracted from the theoretical equilibrium Δ_{63} and Δ_{64} values, respectively, to yield AFFs for calcite at 33.7 ^{o}C ($\Delta^*_{63\text{-}47} = 0.1949$ ‰; $\Delta^*_{64\text{-}48} = 0.1308$ ‰) and 600 ^{o}C ($\Delta^*_{63\text{-}47} = 0.1881$ ‰; $\Delta^*_{64\text{-}48} = 0.1300$ ‰) using Equations A1 and A2

$$\Delta^*_{63\text{-}47} = \Delta_{47\ \text{I-CDES}} - \Delta_{63} \qquad \text{Equation A1}$$

$$\Delta^*_{63\text{-}47} = \Delta_{48\ \text{CDES 90}} - \Delta_{64} \qquad \text{Equation A2}$$

where $\Delta^*_{63\text{-}47}$ and $\Delta^*_{63\text{-}47}$ are the AFFs. Devils Hole calcite was used in construction of the coupled carbonate clumped isotope relationship because it is assumed to have precipitated near isotopic equilibrium due to extremely slow precipitation rate (0.1-0.8 μm year-1), low calcite saturation index (0.16-0.21) and a stable temperature of 33.7 (±0.8) ºC throughout the Holocene.[15,17,18] The pooled average of ETH-1 and ETH-2 was used because their Δ_{47} and Δ_{48} values were statistically indistinguishable, and both have a known equilibration temperature of 600 ºC.[16] Additionally, samples equilibrated at high temperatures are much less likely to have detectable kinetic biases due to faster exchange of isotopes among isotopologues and decreased time to reach isotopic equilibrium.

Linear regressions were made for $\Delta^*_{63\text{-}47}$ versus Δ_{63}, and $\Delta^*_{64\text{-}48}$ versus Δ_{64} for 33.7 ºC and 600 ºC (Figure A1). The slope and intercept from these regressions were used to calculate $\Delta^*_{63\text{-}47}$ and $\Delta^*_{64\text{-}48}$ for 0-1000 ºC (Table 8), using Equations 13 and 14.

$$\Delta^*_{63\text{-}47} = 0.0193 \times \Delta_{63} + 0.1878 \qquad \text{Equation A3}$$

$$\Delta^*_{64\text{-}48} = 0.0077 \times \Delta_{64} + 0.1300 \qquad \text{Equation A4}$$

The relationship between precipitation temperature and $\Delta^*_{63\text{-}47}$ from 0-600 ºC (Figure A1c) is represented by equation A4 (r^2 =1). The relationship between precipitation temperature and $\Delta^*_{64\text{-}48}$ was split into two ranges to acquire a more accurate fit, with 0-300 ºC (Figure A1d) represented by equation A5 (r^2 = 1), and 300-1000 ºC (Figure A1e) represented by Equation A6 (r^2 = 1). Equations 15-17 use temperature in degrees Celsius.

Equation A5

$$\Delta^*_{63\text{-}47} = [0.1968 \pm (1.805 \times 10^{-5})] - [(6.111 \times 10^{-5}) \pm (5.894 \times 10^{-7})]T + [(1.922 \times 10^{-7}) \pm (4.733 \times 10^{-9})]T^2 - [(2.965 \times 10^{-10}) \pm (1.304 \times 10^{-11})]T^3 + [(1.762 \times 10^{-13}) \pm (1.126 \times 10^{-14})]T^4$$

Equation A6

$$\Delta^*_{64\text{-}48} = [0.1312 \pm (7.348 \times 10^{-7})] - [(1.266 \times 10^{-5}) \pm (4.736 \times 10^{-8})]T + [(6.890 \times 10^{-8}) \pm (8.299 \times 10^{-10})]T^2 - [(2.029 \times 10^{-10}) \pm (4{,}756 \times 10^{-12})]T^3 + [(2.428 \times 10^{-13}) \pm (8.335 \times 10^{-15})]T^4$$

Equation A7

$$\Delta^*_{64\text{-}48} = [0.1305 \pm (2.101 \times 10^{-5})] - [(2.165 \times 10^{-6}) \pm (1.516 \times 10^{-7})]T + [(4.011 \times 10^{-9}) \pm (3.858 \times 10^{-10})]T^2 - [(3.377 \times 10^{-12}) \pm (4.135 \times 10^{-13})]T^3 + [(1.072 \times 10^{-15}) \pm (1.587 \times 10^{-16})]T^4$$

The relationship between $\Delta^*_{63\text{-}47}$ and $\Delta^*_{64\text{-}48}$ is represented by equation A8.

Equation A8

$\Delta^*_{64\text{-}48} = (0.3964 \pm 0.0033) + (-2.898 \pm 0.0340)\,\Delta^*_{63\text{-}47} + (7.88 \pm 0.0887)\,\Delta^*_{63\text{-}47}{}^2$

For samples with unknown precipitation temperature, $\Delta^*_{63\text{-}47}$ and $\Delta^*_{64\text{-}48}$ can be calculated using equations A9 and A10 (Figure A1a, b).

$\Delta^*_{63\text{-}47} = 0.0190 \times \Delta_{47\ \text{I-CDES}} + 0.1842$ Equation A9

$\Delta^*_{64\text{-}48} = 0.0077 \times \Delta_{48\ \text{CDES 90}} + 0.1290$ Equation A10

Equations A11 and A12 may be used to calculate Δ_{63} and Δ_{64} from Δ_{47} and Δ_{48} values (Figure A1c, d).

Equation A11

$\Delta_{63} = (-0.1845 \pm 0.0007) + (0.9839 \pm 0.0078)\Delta_{47\ \text{I-CDES}} + (-0.0121 \pm 0.0299)\Delta_{47\ \text{I-CDES}}{}^2 + (0.0207 \pm 0.0483)\,\Delta_{47\ \text{I-CDES}}{}^3 + (-0.0125 \pm 0.0281)\Delta_{47\ \text{I-CDES}}{}^4$

Equation A12

$\Delta_{64} = (-0.1377 \pm 0.0048) + (1.166 \pm 0.0981)\Delta_{48\ \text{CDES 90}} + (-1.267 \pm 0.7306)\Delta_{488\ \text{CDES 90}}{}^2 + (4.007 \pm 2.363)\Delta_{48\ \text{CDES 90}}{}^3 + (-4.645 \pm 2.807)\Delta_{488\ \text{CDES 90}}{}^4$

The $\Delta^*_{63\text{-}47}$ versus Δ_{63} slope of 0.0193 determined here (Figure A1a) differs by -0.0112 ‰ from the model predicted slope from Guo et al.[12] of 0.0305. The model calculated the dependence based on carbonates with $\delta^{13}C = 0$ and $\delta^{18}O = 0$, however, this may not be the source of the offset because the slope is only predicted to change by ~0.002 ‰ and ~-0.0005 ‰ for a 50 ‰ increase in $\delta^{13}C$ and $\delta^{18}O$, respectively.[12] The slope offset may in-part arise from approximations made in the model calculations for isotopologues containing ^{17}O, and uncertainty in the slope determined in this study from the use of only two temperatures.

Fiebig et al.[19] used a similar method to determine AFFs at 600 °C. Our 600 °C $\Delta^*_{63\text{-}47}$ and $\Delta^*_{64\text{-}48}$ values differed by 0.008 ‰ and 0.006 ‰, respectively, from their values of 0.196 ‰ and 0.136 ‰. Because the calculation of AFFs relies on the long term ETH-1 and ETH-2 Δ_{47} and Δ_{48} values, the difference in AFFs is equivalent to the difference in the long term pooled average ETH-1 and ETH-2 Δ_{47} and Δ_{48} values from this study (pooled average ETH-1 and ETH-2 $\Delta_{47\ \text{I-CDES}} = 0.206 \pm 0.0006$ ‰, n = 1497; $\Delta_{48\ \text{CDES 90}} = 0.132 \pm 0.002$ ‰, n = 903) versus Fiebig et al.[19] (pooled average ETH-1 and ETH-2 $\Delta_{47\ \text{I-CDES}} = 0.214 \pm 0.005$ ‰, n = 37; $\Delta_{48\ \text{CDES 90}} = 0.138 \pm 0.015$ ‰, n = 37).

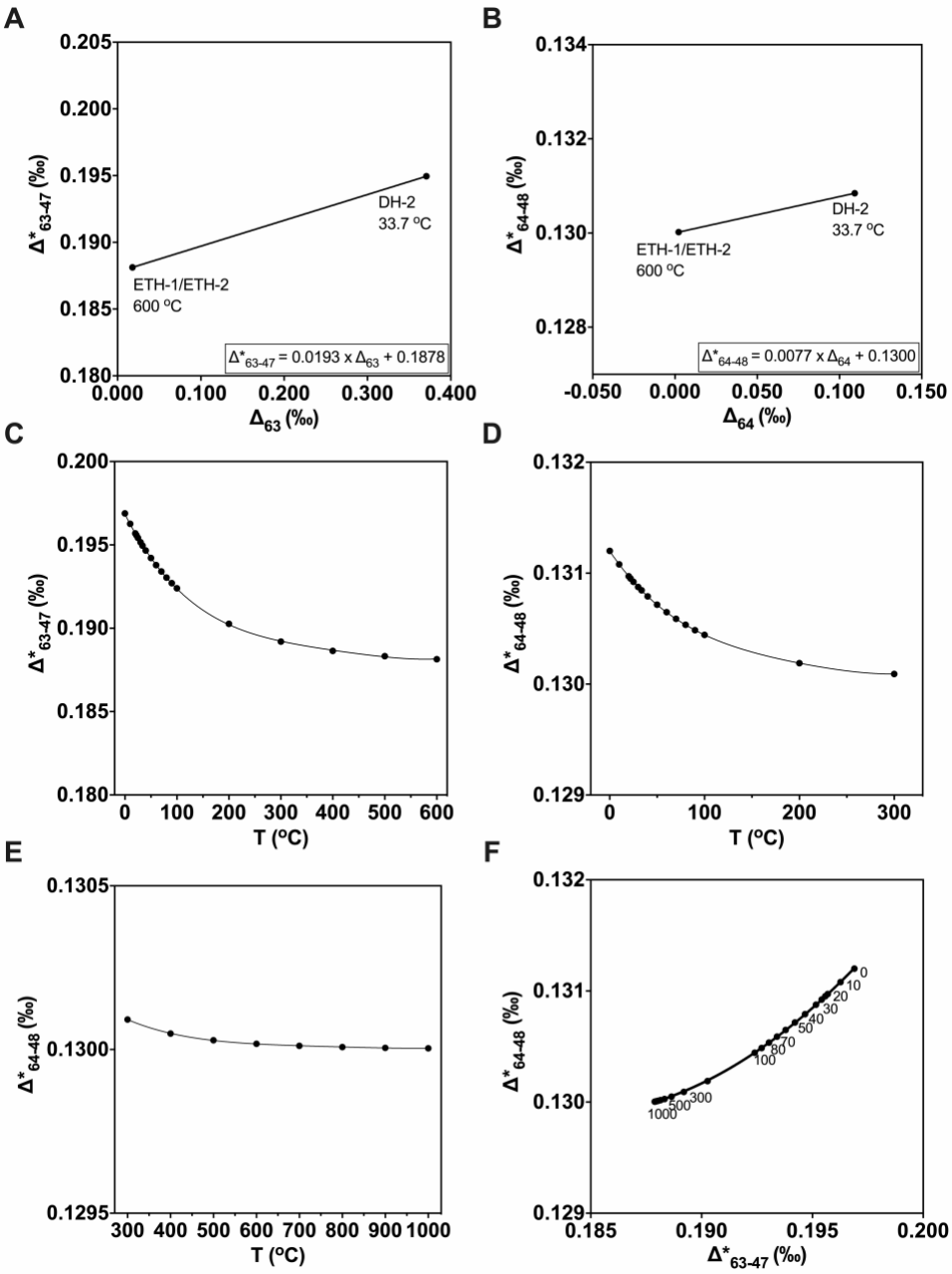

Figure A1. Constraints on acid digestion fractionation factors. **A)** Regression for the acid digestion fractionation factor, $\Delta^*_{63\text{-}47}$, versus theoretical Δ_{63}[13,14]. **B)** Regression for the acid digestion fractionation factor, $\Delta^*_{64\text{-}48}$ versus theoretical Δ_{64}[13,14]. **C)** Regression for acid digestion fractionation factor, $\Delta^*_{63\text{-}47}$, versus precipitation temperature (°C), where $r^2 = 0.99$. **D)** Regression for the acid digestion fractionation factor, $\Delta^*_{64\text{-}48}$ versus precipitation temperature from 0-300 °C ($r^2 = 1$) **E)** and from 300-1000 °C ($r^2 = 0.9998$). **F)** Regression for acid digestion fractionation factors, $\Delta^*_{64\text{-}48}$ versus $\Delta^*_{63\text{-}47}$ ($r^2 = 1$). Numbers on regression indicate temperature in Celsius.

1. Correa-Quezada, R., Cueva-Rodríguez, L., Álvarez-García, J. & del Río-Rama, M. de la C. Application of the Kernel Density Function for the Analysis of Regional Growth and Convergence in the Service Sector through Productivity. *Mathematics* **8**, 1234 (2020).
2. Seaman, D. E. & Powell, R. A. An Evaluation of the Accuracy of Kernel Density Estimators for Home Range Analysis. *Ecology* **77**, 2075–2085 (1996).
3. Pulkkinen, S. Nonlinear kernel density principal component analysis with application to climate data. *Stat Comput* **26**, 471–492 (2016).
4. Wahiduzzaman, M. & Yeasmin, A. A kernel density estimation approach of North Indian Ocean tropical cyclone formation and the association with convective available potential energy and equivalent potential temperature. *Meteorol Atmos Phys* **132**, 603–612 (2020).
5. Lee, W. J., Mendis, G. P., Triebe, M. J. & Sutherland, J. W. Monitoring of a machining process using kernel principal component analysis and kernel density estimation. *J Intell Manuf* **31**, 1175–1189 (2020).
6. R Core Team. R: A language and environment for statistical computing. (2021).
7. Sheather, S. J. & Jones, M. C. A Reliable Data-Based Bandwidth Selection Method for Kernel Density Estimation. *Journal of the Royal Statistical Society: Series B (Methodological)* **53**, 683–690 (1991).
8. Deng, H. & Wickham, H. Density estimation in R. (2011).
9. J Pinheiro, Bates, D., DebRoy, S., Sarkar, D. & R Core Team. nlme: Linear and nonlinear mixed effects models. (2021).
10. Upadhyay, D. *et al.* Carbonate clumped isotope analysis (Δ_{47}) of 21 carbonate standards determined via gas-source isotope-ratio mass spectrometry on four instrumental configurations using carbonate-based standardization and multiyear data sets. *Rapid Commun Mass Spectrom* **35**, (2021).
11. Lenth, R. V. emmeans: Estimated marginal means, aka least-squares means. (2021).
12. Guo, W., Mosenfelder, J. L., Goddard, W. A. & Eiler, J. M. Isotopic fractionations associated with phosphoric acid digestion of carbonate minerals: Insights from first-principles theoretical modeling and clumped isotope measurements. *Geochimica et Cosmochimica Acta* **73**, 7203–7225 (2009).
13. Hill, P. S., Tripati, A. K. & Schauble, E. A. Theoretical constraints on the effects of pH, salinity, and temperature on clumped isotope signatures of dissolved inorganic carbon species and precipitating carbonate minerals. *Geochimica et Cosmochimica Acta* **125**, 610–652 (2014).
14. Tripati, A. K. *et al.* Beyond temperature: Clumped isotope signatures in dissolved inorganic carbon species and the influence of solution chemistry on carbonate mineral composition. *Geochimica et Cosmochimica Acta* **166**, 344–371 (2015).

15. Winograd, I. J. *et al.* Continuous 500,000-Year Climate Record from Vein Calcite in Devils Hole, Nevada. *Science* **258**, 255–260 (1992).
16. Bernasconi, S. M. *et al.* Reducing Uncertainties in Carbonate Clumped Isotope Analysis Through Consistent Carbonate-Based Standardization. *Geochem. Geophys. Geosyst.* **19**, 2895–2914 (2018).
17. Coplen, T. B. Calibration of the calcite–water oxygen-isotope geothermometer at Devils Hole, Nevada, a natural laboratory. *Geochimica et Cosmochimica Acta* **71**, 3948–3957 (2007).
18. Winograd, I. J. *et al.* Devils Hole, Nevada, δ^{18}O record extended to the mid-Holocene. *Quat. res.* **66**, 202–212 (2006).
19. Fiebig, J. *et al.* Combined high-precision Δ48 and Δ47 analysis of carbonates. *Chemical Geology* **522**, 186–191 (2019).